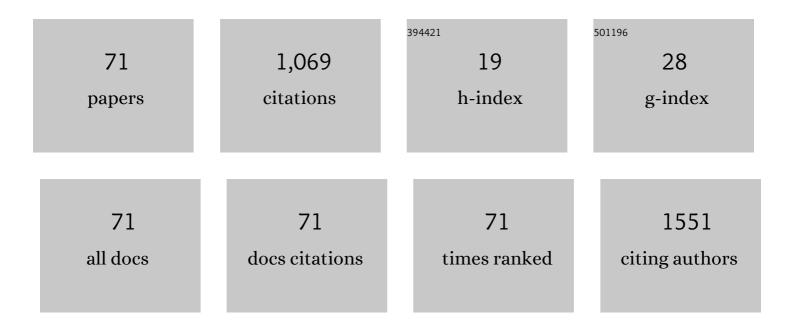
List of Publications by Year in descending order

Source: https://exaly.com/author-pdf/9106854/publications.pdf Version: 2024-02-01



#	Article	IF	CITATIONS
1	WS2-decorated ZnO nanorods and enhanced ultraviolet emission. Materials Letters, 2022, 306, 130880.	2.6	6
2	Effects of experimental conditions on the growth of g–C ₃ N ₄ nanocones by plasma sputtering reaction deposition. Functional Materials Letters, 2022, 15, .	1.2	1
3	WS2 coating and Au nanoparticle decoration of ZnO nanorods for improving light-activated NO2 sensing. Applied Surface Science, 2022, 584, 152508.	6.1	16
4	Synthesis of Plasmonic Z-Scheme g-C3N4/W18O49 Nanocone Arrays with Enhanced Charge Separation. Journal of Physical Chemistry C, 2021, 125, 4205-4210.	3.1	6
5	Auâ€Decorated ZnO Nanorod Powder and Its Application in Photodegradation of Organic Pollutants in the Visible Region. Physica Status Solidi (A) Applications and Materials Science, 2021, 218, 2000737.	1.8	6
6	CuO: Synthesis in a Highly Excited Oxygen-Copper Plasma and Decoration of ZnO Nanorods for Enhanced Photocatalysis. Journal of Physical Chemistry C, 2021, 125, 9119-9128.	3.1	11
7	ZnS Covering of ZnO Nanorods for Enhancing UV Emission from ZnO. Journal of Physical Chemistry C, 2021, 125, 13732-13740.	3.1	9
8	Highâ€Visibleâ€Light Photocatalytic Activity of ZnO–Au Nanocomposites Synthesized by a Controlled Hydrothermal Method. Physica Status Solidi (A) Applications and Materials Science, 2021, 218, 2100150.	1.8	5
9	Structure and optical properties of ZrxHf1-xO2 films deposited by pulsed laser co-ablation of Zr and Hf targets with the assistance of oxygen plasma. Ceramics International, 2021, 48, 587-587.	4.8	2
10	Radio-frequency epsilon-negative property and diamagnetic response of percolative Ag/CCTO metacomposites. Scripta Materialia, 2021, 203, 114067.	5.2	33
11	ZnO:Au nanocomposites with high photocatalytic activity prepared by liquid-phase pulsed laser ablation. Optics and Laser Technology, 2021, 133, 106533.	4.6	15
12	Graphene–Carbon Black/CaCu ₃ Ti ₄ O ₁₂ Ternary Metacomposites toward a Tunable and Weakly ε-Negative Property at the Radio-Frequency Region. Journal of Physical Chemistry C, 2020, 124, 23361-23367.	3.1	30
13	ZnO colloids and ZnO nanoparticles synthesized by pulsed laser ablation of zinc powders in water. Materials Science in Semiconductor Processing, 2020, 109, 104918.	4.0	20
14	Large Enhancement and Its Mechanism of Ultraviolet Emission from ZnO Nanorod Arrays at Room and Low Temperatures by Covering with Ti Coatings. Journal of Physical Chemistry C, 2020, 124, 4827-4834.	3.1	6
15	Sandwiched CdS/Au/ZnO Nanorods with Enhanced Ultraviolet and Visible Photochemical and Photoelectrochemical Properties via Semiconductor and Metal Cosensitizing. Journal of Physical Chemistry C, 2020, 124, 10941-10950.	3.1	13
16	Spatial confinement of laser-induced plasma by laser-induced and obstacle-reflected shock wave and its effect on optical emission of laser-induced plasma. AIP Advances, 2019, 9, .	1.3	7
17	Tailoring of optical and electrical properties of transparent and conductive Al-doped ZnO films by adjustment of Al concentration. Materials Science in Semiconductor Processing, 2018, 74, 147-153.	4.0	23
18	Effects of the experimental conditions on the growth of crystalline NiCx nanorods via pulsed laser deposition accompanied by N2 annealing. Applied Surface Science, 2017, 403, 670-676.	6.1	2

#	Article	IF	CITATIONS
19	Spectroscopic studies of the plasma for the preparation of Al-N co-doped ZnO films. Spectrochimica Acta, Part B: Atomic Spectroscopy, 2017, 131, 48-57.	2.9	1
20	Size-controllable growth of ZnO nanorods on Si substrate. Superlattices and Microstructures, 2017, 101, 469-479.	3.1	12
21	Enhanced light absorption and quenched photoluminescence resulting in photoactive poly(3-hexyl-thiophene)-covered ZnO/TiO 2 nanotubes for high light harvesting efficiency. Solar Energy Materials and Solar Cells, 2017, 162, 47-54.	6.2	5
22	High Visible Photoelectrochemical Activity of Ag Nanoparticle-Sandwiched CdS/Ag/ZnO Nanorods. ACS Applied Materials & Interfaces, 2017, 9, 658-667.	8.0	86
23	Engineering of optical and electrical properties of ZnO by non-equilibrium thermal processing: The role of zinc interstitials and zinc vacancies. Journal of Applied Physics, 2017, 122, 035303.	2.5	17
24	The electro-optic mechanism and infrared switching dynamic of the hybrid multilayer VO2/Al:ZnO heterojunctions. Scientific Reports, 2017, 7, 4425.	3.3	20
25	Enhanced visible photoelectrochemical properties of ZnO/CdS core/shell nanorods and their correlation with improved optical properties. Applied Physics Letters, 2016, 109, 203106.	3.3	15
26	Enhanced Photoelectrochemical Activity of ZnO-Coated TiO2 Nanotubes and Its Dependence on ZnO Coating Thickness. Nanoscale Research Letters, 2016, 11, 104.	5.7	35
27	Spectroscopic characterization of the plasmas formed during the deposition of ZnO and Al-doped ZnO films by plasma-assisted pulsed laser deposition. Spectrochimica Acta, Part B: Atomic Spectroscopy, 2016, 125, 18-24.	2.9	13
28	Multi-band luminescent ZnO/ZnSe core/shell nanorods and their temperature-dependent photoluminescence. RSC Advances, 2016, 6, 98413-98421.	3.6	11
29	Enhanced charge separation of vertically aligned CdS/g-C ₃ N ₄ heterojunction nanocone arrays and corresponding mechanisms. Journal of Materials Chemistry C, 2016, 4, 7501-7507.	5.5	26
30	Polycrystalline ZnTe thin film on silicon synthesized by pulsed laser deposition and subsequent pulsed laser melting. Materials Research Express, 2016, 3, 036403.	1.6	8
31	Spectral assignments in the infrared absorption region and anomalous thermal hysteresis in the interband electronic transition of vanadium dioxide films. Physical Chemistry Chemical Physics, 2016, 18, 6239-6246.	2.8	13
32	Blue shift in absorption edge and widening of band gap of ZnO by Al doping and Al–N co-doping. Journal of Alloys and Compounds, 2015, 644, 528-533.	5.5	49
33	Composition and bandgap control of Al _x Ga _{1â^'x} N films synthesized by plasma-assisted pulsed laser deposition. Journal of Materials Chemistry C, 2015, 3, 5307-5315.	5.5	10
34	Highly transparent and conductive Al-doped ZnO films synthesized by pulsed laser co-ablation of Zn and Al targets assisted by oxygen plasma. Journal of Alloys and Compounds, 2015, 626, 415-420.	5.5	50
35	Extended photoresponse of ZnO/CdS core/shell nanorods to solar radiation and related mechanisms. Solar Energy Materials and Solar Cells, 2015, 137, 169-174.	6.2	25
36	Spectroscopic characterization of the plasma generated during the deposition of Al _{<i>x</i>} Ga _{1â^'<i>x</i>} N films by pulsed laser co-ablation of Al and GaAs targets in electron cyclotron resonance nitrogen plasma. Journal Physics D: Applied Physics, 2015, 48, 245203.	2.8	1

#	Article	IF	CITATIONS
37	Manipulations from oxygen partial pressure on the higher energy electronic transition and dielectric function of VO ₂ films during a metal–insulator transition process. Journal of Materials Chemistry C, 2015, 3, 5033-5040.	5.5	33
38	Confinement effects of shock waves on laser-induced plasma from a graphite target. Physics of Plasmas, 2015, 22, 063509.	1.9	10
39	Synthesis and characterization of single-crystalline graphitic C ₃ N ₄ nanocones. CrystEngComm, 2015, 17, 512-515.	2.6	10
40	Optical Properties of ZnO Nanorod-Based Heterogeneous Core/Shell Arrays. , 2015, , .		0
41	Formation of diatomic molecular radicals in reactive nitrogen-carbon plasma generated by electron cyclotron resonance discharge and pulsed laser ablation. Physics of Plasmas, 2014, 21, 043512.	1.9	5
42	Photoluminescence enhancement of Si nanocrystals embedded in SiO2 by thermal annealing in air. Applied Surface Science, 2014, 320, 804-809.	6.1	8
43	Optoelectronic properties of ZnO film on silicon after SF ₆ plasma treatment and milliseconds annealing. Applied Physics Letters, 2014, 105, 221903.	3.3	15
44	Extended photo-response of ZnO/CdS core/shell nanorods fabricated by hydrothermal reaction and pulsed laser deposition. Optics Express, 2014, 22, 8617.	3.4	17
45	Enhancement and stability of photoluminescence from Si nanocrystals embedded in a SiO2 matrix by H2-passivation. Applied Surface Science, 2014, 300, 178-183.	6.1	11
46	Extended photoresponse and multi-band luminescence of ZnO/ZnSe core/shell nanorods. Nanoscale Research Letters, 2014, 9, 31.	5.7	19
47	Fabrication and correlation between photoluminescence and photoelectrochemical properties of vertically aligned ZnO coated TiO2 nanotube arrays. Solar Energy Materials and Solar Cells, 2014, 123, 233-238.	6.2	12
48	Enhanced photoelectrochemical activity of vertically aligned ZnO-coated TiO2 nanotubes. Applied Physics Letters, 2014, 104, 053114.	3.3	31
49	Controlled growth of crystalline g-C3N4 nanocone arrays by plasma sputtering reaction deposition. Carbon, 2014, 79, 578-589.	10.3	33
50	High excitation of the species in nitrogen–aluminum plasma generated by electron cyclotron resonance microwave discharge of N2 gas and pulsed laser ablation of Al target. Spectrochimica Acta, Part B: Atomic Spectroscopy, 2014, 101, 226-233.	2.9	6
51	A comparative study of the enhancement of molecular emission in a spatially confined plume through optical emission spectroscopy and probe beam deflection measurements. Spectrochimica Acta, Part B: Atomic Spectroscopy, 2013, 79-80, 44-50.	2.9	14
52	Synthesis, phase transition and optical properties of nanocrystalline titanium dioxide films deposited by plasma assisted reactive pulsed laser deposition. Surface and Coatings Technology, 2013, 231, 180-184.	4.8	9
53	Photoluminescence and low-threshold lasing of ZnO nanorod arrays. Optics Express, 2012, 20, 14857.	3.4	37
54	Transparent polycrystalline monoclinic HfO2 dielectrics prepared by plasma assisted pulsed laser deposition. Journal of Vacuum Science and Technology A: Vacuum, Surfaces and Films, 2012, 30, 011506.	2.1	2

#	Article	IF	CITATIONS
55	Photoluminescence and Lasing Properties of Catalyst-Free ZnO Nanorod Arrays Fabricated by Pulsed Laser Deposition. Journal of Physical Chemistry C, 2012, 116, 2330-2335.	3.1	33
56	Growth of CdS Nanoneedles by Pulsed Laser Deposition. Journal of Electronic Materials, 2012, 41, 1941-1947.	2.2	9
57	Correlation between structure and photoluminescence of c-axis oriented nanocrystalline ZnO films and evolution of photo-generated excitons. Solar Energy Materials and Solar Cells, 2012, 96, 117-123.	6.2	11
58	Infrared and Raman Spectroscopic Studies of Optically Transparent Zirconia (ZrO ₂) Films Deposited by Plasma-Assisted Reactive Pulsed Laser Deposition. Applied Spectroscopy, 2011, 65, 522-527.	2.2	10
59	Spectroscopic Characterization of Plasmas Generated by ECR Microwave Discharge of N ₂ Gas and Pulsed Laser Ablation of a B ₄ C Target. Plasma Processes and Polymers, 2011, 8, 1146-1153.	3.0	4
60	Study on phase separation in a-SiOx for Si nanocrystal formation through the correlation of photoluminescence with structural and optical properties. Applied Surface Science, 2011, 257, 6145-6151.	6.1	19
61	Ab initio calculation of diffusion barriers for Cu adatom hopping on Cu(100) surface and evolution of atomic configurations. Applied Surface Science, 2011, 257, 7507-7515.	6.1	2
62	Self-Assembled Fabrication and Characterization of Vertically Aligned Binary CN Nanocone Arrays. Journal of Electronic Materials, 2010, 39, 381-390.	2.2	5
63	Annealing behaviors of structural, interfacial and optical properties of HfO2 thin films prepared by plasma assisted reactive pulsed laser deposition. Journal of Materials Research, 2010, 25, 680-686.	2.6	9
64	Structure and photoluminescence of c-axis oriented Nnanocrystalline ZnO films synthesized by plasma assisted pulsed laser deposition. , 2010, , .		0
65	Evolution of photoluminescence from Si nanocrystals embedded in a SiO ₂ matrix prepared by reactive pulsed laser deposition. Journal of Materials Research, 2009, 24, 2259-2267.	2.6	3
66	Growth of ZnSe nanowires by pulsed-laser deposition. Journal of Vacuum Science & Technology B, 2007, 25, 1823.	1.3	19
67	Growth of Nanocrystalline ZnSe:N Films by Pulsed Laser Deposition. Journal of Electronic Materials, 2007, 36, 75-80.	2.2	8
68	Arsenic doping for synthesis of nanocrystalline p-type ZnO thin films. Journal of Vacuum Science and Technology A: Vacuum, Surfaces and Films, 2006, 24, 517-520.	2.1	27
69	Synthesis of carbon nitride nanocrystals on Co/Ni-covered substrate by nitrogen-atom-beam-assisted pulsed laser ablation. Journal of Materials Research, 2003, 18, 2552-2555.	2.6	5
70	Raman spectra of nanocrystalline carbon nitride synthesized on cobalt-covered substrate by nitrogen-atom-beam-assisted pulsed laser ablation. Journal of Applied Physics, 2002, 92, 496-500.	2.5	6
71	Photoluminescence and its time evolution of AlN thin films. Physics Letters, Section A: General, Atomic and Solid State Physics, 2001, 280, 381-385.	2.1	19